Dilatometric Study of the Quench and Partitioning Process

E. De Moor[1*], S. Lacroix[2], L. Samek[1], J. Penning[1] and J.G. Speer[3]

[1]*Laboratory for Iron and Steelmaking (LISm), Department of Metallurgy and Materials Science, Ghent University, Technologiepark 903, B-9052 Ghent, Belgium,*
emmanuel.demoor@ugent.be, ludovic.samek@ugent.be
[2]*Arcelor Research Industry Gent, OCAS NV, J. Kennedylaan 3, B-9060 Zelzate, Belgium,*
sophie.lacroix@arcelor.com
[3] *Advanced Steel Processing and Products Research Centre, Colorado School of Mines, Golden 80401, Colorado, USA,*
jspeer@mines.edu

Abstract. A new thermal processing route, Quench and Partitioning (Q&P), has been proposed recently as a way to produce high-strength martensitic steels with good ductility or toughness. It consists of quenching a steel to a suitable temperature and subsequently reheating it to a higher temperature, the so called partitioning temperature. During the latter heat treatment, carbon is rejected from a carbon supersaturated martensitic microstructure into the remaining austenite, stabilizing the latter. The usual formation of carbides on tempering of martensite is suppressed by the presence of Si and/or Al. In the present contribution, the Q&P process is studied by means of dilatometry and differential scanning calorimetry (DSC). The effect of Si and Al on tempering is studied and the implications for Q&P processing are adressed.

1. INTRODUCTION

Increasing passenger car safety regulations and environmental concerns have led to the development and increased use of several types of advanced high strength steel grades (AHSS). A primary goal of the development of AHSS grades has always been the increase of the strength without significant loss in formability. This allows for the production and application of thinner gauged, high strength automotive body parts. The resulting decrease in car body weight leads to reduced fuel consumption and emissions. Namely Dual-Phase (DP) and Transformation Induced Plasticity (TRIP) steel are grades developed for automotive applications.

A fundamentally new steel processing route, called Quench and Partitioning (Q&P), has recently been proposed by Speer *et al.* [1] in order to produce a new type of advanced high strength steel grade. This new concept consists of a two-step process. After reheating in order to obtain a fully austenitic or intercritical microstructure, the steel is quenched to a temperature (QT) which is lower than the martensite start temperature (M_s) but higher than the martensite finish temperature (M_f). Hence, the microstructure at the quench temperature consists of martensite and untransformed austenite. The second step of the process consists of either holding the steel at the QT for a longer time (1-step Q&P) or reheating the steel to a higher temperature, the so-called partitioning temperature (2-step Q&P). After a time, Pt, at that temperature a final quench to room temperature follows. The goal of the second step is to enrich the austenite present at the quench temperature with carbon via carbon depletion of the martensite laths, in order to decrease its M_s temperature so that thermally stable austenite is obtained after the final quenching to room temperature. Alloying with Al, Si and/or P is believed necessary to suppress carbide formation in the austenite and martensite. The use of Si must be restricted for some applications since high-Si steels have poor hot-dip coatability [2]. A (partial) replacement of Si by Al is effective in retarding cementite formation without a detrimental effect on galvanizability [3].

The amount of retained austenite depends on the partitioning time and temperature but is also dependent on the quench temperature since this temperature determines the potential level of carbon enrichment. A methodology has been developed to determine an "optimum" quench temperature assuming that all the carbon is rejected from the martensite into the austenite and that no carbide formation occurs [1,4,5,6,7]. The predicted retained austenite fraction is a maximum at the optimum QT [8].

Mechanical properties obtained after Q&P processing of grades with a typical TRIP sheet steel composition show potential for use in automotive applications such as pillars and anti-intrusion barriers [5]. Very high strength levels are combined with sufficient ductility. Notably higher ductilities are obtained with Q&P processing compared to quench & tempering (Q&T), indicating the potential for general industry applications. Since it is essential for the Q&P process to suppress carbide formation, it is important to know the effect of Si and Al on transition carbide and cementite formation, and their relative abilities to suppress carbides during Q&P. These issues are examined in the present work.

2. EXPERIMENTAL PROCEDURE

Three steel chemical compositions were used in this study as shown in Table 1 including Si, Al and Si/Al modifications. The CMnSiAl steel was included because the CMnAl grade could not be fully austenitized due to the limited temperature of the salt bath. Laboratory castings were prepared as 100kg ingots in a Pfeiffer VSG100 vacuum melting and casting unit, operated under an Ar protective atmosphere. The ingots were cut into blocks of 250mm width, 120mm length and 25mm thickness. The blocks were reheated for 1 hour at a temperature of 1250°C and hot rolled in

3 passes to a final thickness of 3.5 mm. A coiling simulation was performed at 600°C. After pickling the steels were cold rolled to a final thickness of 1mm.

Q&P of the CMnSi and CMnSiAl grade was done using salt baths. Specimens were austenitized for 3 minutes at 900°C, quenched to the optimum quench temperature and partitioned at 300°C during various partitioning times in the range of 10s-900s. The optimum quench temperature was calculated using the approach proposed by Speer *et al.* [1]. A calculated optimum QT of 248°C was obtained for the CMnSi grade and 259°C for the CMnSiAl grade. The CMnAl grade was excluded from this step as it could not be austenitized fully.

Austenite volume fractions were determined with magnetic saturation according to the method proposed by Wirthl *et al.* [9].

	C	Mn	Si	Al	A_{c3}	M_s
CMnSi	0.24	1.61	1.45	0.3	867	378
CMnSiAl	0.25	1.70	0.55	0.69	895	402
CMnAl	0.18	1.56	0.02	1.73	1017	471

Table 1: Chemical compositions of the investigated steel grades (in wt%) and measured transformation temperatures (°C).

4×10×1mm specimens for dilatometry were prepared from the cold rolled sheet by spark erosion. A DIL805A/D Bähr type dilatometer in quenching mode was used operating under vacuum (10^{-4} mbar). Quenching was done with He gas. Hollow push rods were used allowing high quenching rates in order to avoid ferrite/pearlite and bainite formation. Specimens were fully reaustenitized, quenched to room temperature and reheated to 600°C at 10, 20, 50 and 100°C/min to study the tempering behavior. The measured transformation temperatures are given in Table 1. Carbide suppression being of key importance for the Q&P process, this approach has been used for the detection of transition carbide formation and assessment of the effect of Si and Al on this process.

Differential scanning calorimetry (DSC) was performed using a Netzsch 404C apparatus. Calibration was performed by measuring the well-established melting points of high purity indium, tin, zinc, gold and nickel. Pt pans with an Al_2O_3 layer were used. To prevent oxidation, N_2 gas was used at a flow rate of 50ml/min. An empty pan was used as a reference. The baseline was determined by running the same program with 2 empty crucibles. The CMnSi and CMnAl grade were used to study the effect of Si and Al separately. The mass of the specimens varied between 20 and 70mg. Prior to DSC, the samples were fully austenitized and quenched to room temperature in a dilatometer at temperatures sufficient for full austenitization of the CMnAl grade. The DSC samples were cut from the dilatometer samples with a water cooled grinding disc. Tempering was studied by heating the samples from room temperature to 600°C in the DSC at heating rates of 5, 10, 20 and 30°C/min.

To study Q&P microstructure evolution and carbide formation, Transmission Electron Microscopy (TEM) was performed with a Philips EM 420 operating at 120kV. The CMnSi and CMnSiAl grade, both fully austenitized, quenched to their calculated optimum QT and partitioned 120s at 300°C, were studied. Partitioning time and temperature were chosen so as to give a maximal amount of retained austenite. Thin foils were prepared by first thinning to 70 µm using 1200 grit SiC grinding paper. Discs of 3 mm diameter were cut from this thinned sheet and electropolished in a Struers Tenupol jet polisher using a solution of 95% perchloric acid and 5% acetic acid operating at 32V and a temperature of 13°C for 50s.

3. RETAINED AUSTENITE OBTAINED VIA Q&P FOR A CMnSi AND CMnSiAl GRADE

Retained austenite volume fractions obtained via Q&P processing for the CMnSi and CMnSiAl grades are given in Figure 1. For comparison, the amount of austenite present after reaustenitization and water quenching is also shown. Comparable amounts of retained austenite at room temperature are predicted to be present at the optimum quench temperature in the two steels: 23vol% for the CMnSi and 24vol% for the CMnSiAl. An optimum partitioning time of 120s is observed for both grades. Higher amounts are retained in the CMnSi grade than in the CMnSiAl grade for all partitioning times.

TEM thin foils were prepared from the samples partitioned for 120s. Representative mircographs are shown in Figure 2. Figure 2a shows the microstructure obtained for the CMnSiAl grade consisting of martensitic laths and thin, film-like retained austenite as shown in the dark field image in Figure 2b. A high dislocation density is observed. The fine martensitic laths show few transition carbides (Figure 2a). However, in the coarser laths transition carbide precipitation is more prevalent as shown in Figure 2c and Figure 2d. More precipitates seem to be present in the CMnSiAl than in the CMnSi grade (Figure 2d). In an effort to better quantify this observation, the intercarbide spacing was determined from the two microstructures by counting the intersections with a reference line perpendicular to the carbide habit. The results indicated an approximate spacing of 190µm in the CMnSiAl grade and 310µm for the CMnSi grade. Better counting statistics and incorporation of stereological effects would be helpful to quantify the intercarbide spacing more accurately, however.

The absence of transition carbides in the finer martensitic laths may suggest that the martensite is rapidly decarburized. It also shows that the effectiveness of C-enrichment of the austenite via Q&P may be controlled by the lath dimensions and thus diffusion distance. Clearly the transition carbide precipitation behavior in the martensite is important in these steels; thus follow-up tempering studies were used to examine further the effects of Si and Al.
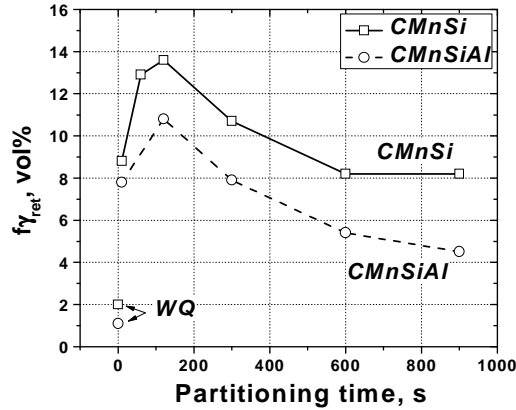
Figure 1: Volume fractions of retained austenite obtained via Q&P processing for the CMnSi and CMnSiAl grades. The samples were fully reaustenitized, quenched to the optimum quench temperature and partitioned at 300°C for 10-900s. For comparison, the austenite fractions, retained after reheating and subsequent water quenching (WQ) are also indicated.

4. INFLUENCE OF Si AND Al ON CARBIDE FORMATION

Tempering reactions have been the subject of intensive investigation for more than 50 years [e.g.10]. However, the influence that cementite-suppressing alloying additions have on transition carbide formation has received less attention [11,12]. This may be related to the fact that transition carbides usually do not have the same detrimental effect on mechanical properties that are found with cementite [13,14]. Although the influence of Si on retarding cementite precipitation has been studied extensively [15,16,17,18], only a few studies have considered the influence of Al [19,20].

Dilatometry and differential scanning calorimetry (DSC) are complementary techniques for the study of the martensite tempering [21,22,23]. A DSC run and the derivative of the change in length obtained for the CMnAl grade at a heating rate of 20°C/min are shown in Figure 3. Similar results were obtained for all grades and heating rates.

As shown in Figure 3, the DSC results suggest that 5 events occur during heating. The activation energies for those events were determined with the modified Kissinger-like method [24,25], based on the equation:

$$\ln \frac{T_{f'}^2}{\phi} = \frac{E}{RT_{f'}} + \ln(\frac{E}{R}) - \ln(A)$$

[1]

Where E is the activation energy in J/mol, A is the pre-exponential factor, $T_{f'}$ is the temperature at which the maximum reaction rate occurs [24] corresponding to a certain fraction (f') of phase transformed and ϕ is the heating rate in K/min. The results are shown in Table 2. The five events are characterized as likely involving carbon segregation and clustering, ε/η precipitation, γ_{ret} decomposition and cementite formation. An explanation for this interpretation is provided in the following paragraphs.

An activation energy of about 56-58kJ/mol was obtained for the first event. There was no significant effect of alloying on the activation energy and no significant length change in the dilatometric signal was observed for this stage. This event might be related to *dislocation pinning and clustering*. However, slightly higher activation energies for Cottrell atmosphere formation and clustering are usually reported for this process, namely 79-85kJ/mol [26], similar to the activation energy for carbon diffusion in a bcc iron lattice (84kJ/mol [27]).

The activation energies for the second event are 127kJ/mol for the CMnSi grade and 116kJ/mol for the CMnAl grade based on the observed DSC peak positions. The replacement of Si by Al results in a decrease in activation energy. A decrease of specific length was observed for all compositions in this temperature range. Activation energies of 111-142kJ/mol along with length decreases were reported by Morra *et al.* for Fe-1%C grades [23] and were related to the precipitation of *ε and/or η transition carbides*. The activation energies are intermediate between those for diffusion of carbon in bcc iron (80kJ/mol) and for diffusion of iron along dislocations (pipe-diffusion, 152kJ/mol). Dislocations are expected to be present to accommodate the misfit between the transition carbide and the matrix.

King and Glover [11] found that the activation energy for the first stage of tempering is influenced by carbon content and increases by 35.56kJ/mol per wt% C. This predicts a difference of 2kJ/mol due to the different carbon levels in the present steels. Si reportedly increases the activation energy by 10kJ/mol per wt% Si in a 1.1%C steel [11]. This was assumed to be related to an increase of the thermodynamic activity coefficient γ_C of the dissolved carbon and the effect on the lattice spacing [11]. Si decreases the lattice spacing of α iron causing an increase in the lattice strains associated with the precipitation of ε-carbide [11].

a)

b)

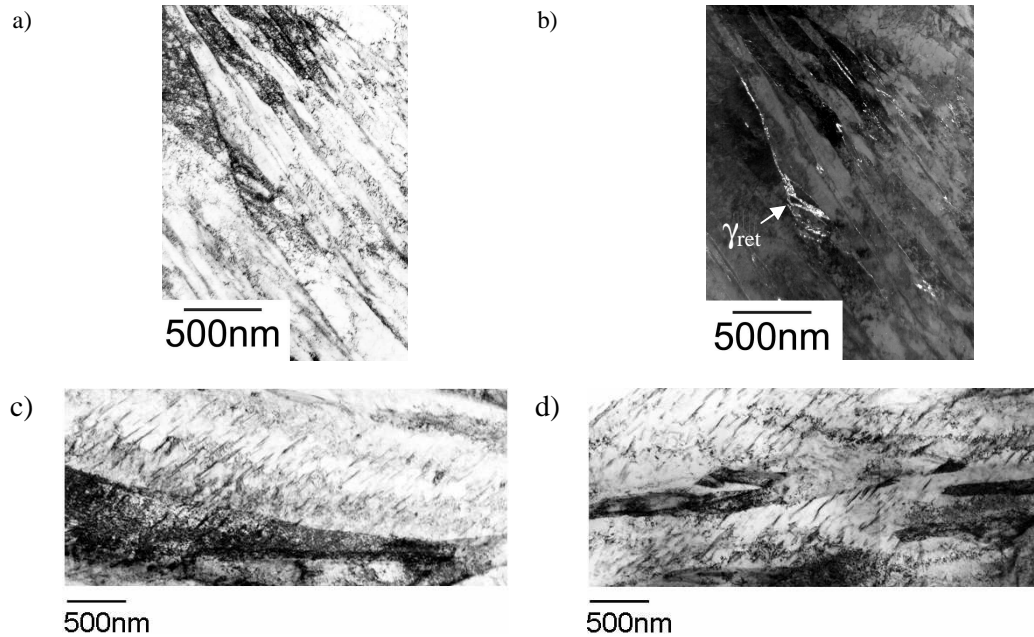γ_{ret}

500nm

500nm

c)

d)

500nm

500nm

Figure 2: Representative micrographs of the CMnSi and CMnSiAl grades after Q&P processing. The steels were fully austenitized, quenched to the calculated optimum QT and partitioned at 300°C for 120s. a) BF image of the CMnSiAl Q&P microstructure showing fine martensitic laths with high dislocation density b) DF image revealing fine thin-film retained austenite c) transition carbides observed in the coarser laths in the CMnSiAl grade d) transition carbides in the coarser laths in the CMnSi grade; a larger intercarbide spacing is observed as compared to the CMnSiAl grade.

As indicated by Leslie *et al.* [19], Si increases the activity coefficient of carbon in ferrite, while Al decreases the coefficient. The effect of Al on the lattice spacings is not reported in the literature. Al is not a solid solution strengthening element, unlike Si.

It is important to notice that nucleation sites for transition carbides might already be present after quenching and thus be present before the DSC run. This makes the experimental determination of the activation energy for the formation of the precipitates more difficult. The measured activation energy might be the activation energy for the growth of the precipitates more than an activation energy for nucleation+growth. This issue might be especially relevant in the present case. Since the CMnAl grade has a significantly high M_s temperature (Table 1), ε/η nuclei are likely to form during cooling. Thus, the activation energy measured subsequently might not fully account for nucleation. Since there is an important difference in M_s temperatures between the CMnSi and CMnAl grades, this effect might also contribute to the lower activation energy found for the CMnAl grade.

The third event is associated with a significant release of heat and an increase in length suggesting *decomposition of retained austenite into a ferrite+carbide mixture*. The values for the activation energies are 124kJ/mol for the CMnAl grade and 202kJ/mol for the CMnSi grade. Owen [15] found activation energies for the second stage of tempering in the range of 113-174kJ/mol. He concluded that the second stage of tempering is carbon diffusion controlled and attributed the retardation of decomposition by Si addition to the influence of Si on the carbon diffusion process. Morra also suggested interface controlled growth, referring to the kinetic analysis (140kJ/mol) for the $\gamma \rightarrow \alpha$ transformation in Fe-Mn alloys [23].

The fourth event exhibits a pronounced length decrease and heat release and is related to the *precipitation of cementite*. The values for the activation energies obtained are 233kJ/mol for the CMnSi grade and 245kJ/mol for the CMnAl grade. Owen found an activation energy of 227 kJ/mol at this stage for a Si-containing steel, in good agreement with the present result. A clear retardation of cementite precipitation by Si was found and was attributed to the build-up of Si in front of the advancing cementite/matrix interface [15]. Since Si has little solubility in cementite, it is rejected by a growing cementite particle causing an enrichment of Si at the interface. For the precipitation to continue, Si must diffuse away from the interface and carbon needs to diffuse in the opposite direction (from the matrix to the interface). At low Si concentrations the process is controlled by the diffusion of carbon, but at higher Si levels, the process is Si diffusion controlled. The activation energy for Si diffusion in bcc iron is reported to be 229 kJ/mol [29]. This supports the theory proposed by Owen since the activation energy for cementite precipitation was found to be 227 kJ/mol [15] and 233 kJ/mol in the present study. The build up of Si at a ferrite/cementite interface has been verified experimentally by means of Field Ion Microscopy [18].
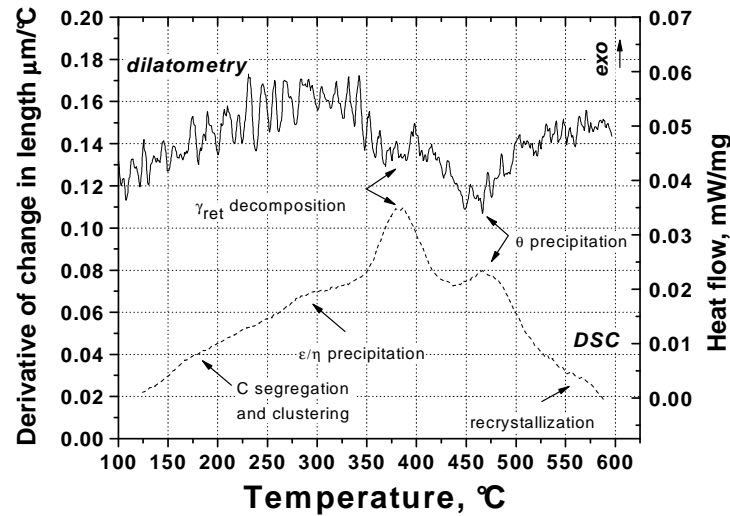
Figure 3: Derivative of the dilatometric change in length (left axis) and DSC heat flow (right axis) obtained for the CMnAl grade. The specimen was fully reaustenitized, quenched to room temperature and reheated to 600°C at 20°C/min. The DSC curve shows 5 events corresponding to the pre-precipitation and 4 tempering stages. The direction of heat flow for exothermic reactions is indicated.

The replacement of Si by Al apparently increases the temperature at which the process occurs and thus the activation energy for cementite precipitation. As is the case for Si, Al has no significant solubility in cementite [19]. Hence, for a cementite precipitate to grow, it has to reject the Al. A similar mechanism as proposed by Owen may be acting. This hypothesis is supported by the activation energy of 245kJ/mol, obtained for the CMnAl grade which is close to the activation energy for the diffusion of Al in bcc iron (241kJ/mol). It should be noted that this activation energy is higher than the activation energy for Si diffusion in bcc iron. The increased activation energy might explain the more effective retardation of cementite formation by Al compared to Si. One might question the greater retardation of cementite formation when alloying with Al, which contradicts the observed reduced activation energy for γ_{ret} decomposition. It should be noted that the exact mechanism by which the decomposition of the retained austenite occurs is not well known, and alloying effects may be different depending on the rate controlling process of interest. Further work is clearly needed in this area, but one hypothesis is that the strong ferrite stabilizing aspect of Al-alloying may drive austenite decomposition [28], while the diffusivity/solubility (in θ) controls cementite precipitation within the martensite.

The last event is associated with a heat release and a length decrease. This event might be related to *recovery* of the martensite. The activation energy could only be determined for the CMnSi grade and amounts 259kJ/mol. The diffusion of iron in bcc iron is reported to have an activation energy of 241 kJ/mol. This suggests that iron diffusion is the rate controlling process as expected for recovery.

	C clustering	ε/η	γ_{ret} decomp	θ	Recrystallization
CMnSi	56	127	202	233	259
CMnAl	58	116	124	245	-

Table 2: Activation energies calculated from the DSC data for the 5 events observed (in kJ/mol).

	diffusion in bcc iron (kJ/mol)	diffusion in fcc iron (kJ/mol)
Fe	241 [29,30]	268 [30], 291 [29]
C	123 [30]	142 [30]
Si	229 [29]	243 [29]
Al	241 [29]	257 [29]

Table 3: Activation energies for element diffusion in bcc and fcc iron (in kJ/mol) [29,30].

5. IMPLICATIONS FOR THE QUENCHING AND PARTITIONING PROCESS

The low activation energy obtained for the precipitation of transition carbides during tempering in the CMnAl grade is consistent with the TEM observations of the Q&P steels, where a smaller intercarbide spacing in the CMnSiAl grade (compared to the CMnSi grade) may reflect ease of nucleation. Better inhibition of transition carbide formation by Si may explain the higher retained austenite fraction obtained after Q&P processing for partitioning times up to 120s and

at 300°C since a tradeoff exists between carbon depletion of the martensite by carbide formation and by carbon rejection into the austenite. After the optimum partitioning time of 120s, austenite decomposition may occur. Al has been shown to decrease the stability of the retained austenite, which may explain the lower retained austenite fractions for the CMnSiAl grade at longer partitioning times.

6. CONCLUSIONS

The main conclusions of the present study are:
-   lower retained austenite volume fractions are obtained for a CMnSiAl steel compared to a CMnSi steel with similar carbon content after Q&P processing.
-   transition carbide formation was not prominent in the *fine* martensite laths for both steels indicating the effectiveness of carbon depletion of the martensite laths by Q&P
-   in the *bigger* laths, transition carbides were present. Transition carbide nuclei may form during quenching in steels with high M_s temperatures.
-   Al may be less effective in retarding transition carbide formation based on the DSC and carbide spacing results here.
-   Al seems to retard cementite formation by a similar mechanism as proposed for Si.
-   A higher activation energy is found for cementite formation in the Al-added grade, in contrast to the lower activation energy associated with transition carbide precipitation.

7. ACKNOWLEDGMENTS

8. REFERENCES

[1] J.G. Speer, D.K. Matlock, B.C. De Cooman and J.G. Schroth, *Acta Materialia*, 51, pp.2611-2622, 2003.
[2] J. Mahieu, S. Claessens and B.C. De Cooman, *Metall. Trans. A - Communications*, 32A, pp.2905-2908, 2001.
[3] J. Mahieu, J. Maki, B.C. De Cooman, M. Fiorucci and S. Claessens, *Mat. Science and Technology*, 19, pp.125-131, 2003.
[4] J.G. Speer, A.M. Streicher, D.K. Matlock, F. Rizzo and G. Krauss, Proc. of Austenite Formation and Decomposition Chicago, Illinois, USA, Nov. 9-12, 2003, pp.502-522.
[5] A.M. Streicher, J.G. Speer, D.K. Matlock and B.C. De Cooman, Proc. of the International Conference Advanced High-Strength Sheet Steels for Automotive Applications, Warrendale, PA, USA, June 6-9 2004, pp.54-62.
[6] J.G. Speer, D.V. Edmonds, F.C. Rizzo and D.K. Matlock, *Current Opinions in Solid State and Materials Science*, 8, pp.219-237, 2004.
[7] J.G. Speer, F.C. Rizzo, D.K. Matlock and D.V. Edmonds, 59th Annual Congress of ABM, Sao Paulo, Brazil, July 19-22 2004, pp. 4824-4836.
[8] J.G. Speer, D.K. Matlock, B.C. De Cooman and J.G. Schroth, *Scripta Materialia*, 50, pp.83-85, 2005.
[9] E.Wirthl, A. Pichler, R. Angerer, P. Stiaszny, K. Hauzenberger, Y.F. Titovets and M. Hackl, INT. Conf. on TRIP-Aided High Strength Ferrous Alloys, Ghent, Belgium, June 19-21 2002, pp.61-64.
[10] G. Krauss, Principles of Heat Treatment of Steels, American Society for Metals, Metals Park, Ohio 44073, USA, 1980.
[11] H.W. King and S.G. Glover, *JISI*, 191, pp.123-132, 1959.
[12] H.W. King and S.G. Glover, *JISI*, 196, pp.281-288, 1960.
[13] M. Sarikaya, A.K. Jhingan and G. Thomas, *Metall. Trans. A*, 14A, pp.1121-1133, 1983.
[14] R.M. Horn and R.O. Ritchie, *Metall. Trans. A*, 9A, pp.1039-1053, 1978.
[15] W.S. Owen, *Trans. ASM*, 46, pp.812-829, 1954.
[16] W.S Owen, *JISI*, 167, pp.117-120, 1951.
[17] J. Gordine and I. Codd, *JISI*, 207, pp.461-467, 1969.
[18] L. Chang and G.D.W. Smith, *Journal de Physique*, C9 supplément au n° 12, pp.397-401, 1984.
[19] W.C. Leslie and G.C. Rauch, *Metall. Trans. A*, 9A, pp.343-349, 1978.
[20] G.M. Michal and J.A. Slane, *Metall. Trans. A*, 17A, pp.1287-1294, 1986.
[21] L. Cheng, C.M. Brakman, B.M. Korevaar and E.J. Mittemeijer, *Metall. Trans. A*, 19A, pp.2415-2426, 1988.
[22] M.J. Van Genderen, M. Isac, A. Böttger and E.J. Mittemeijer, *Metall. Trans. A*, 28A, pp.545-561, 1997.
[23] P.V. Morra, A.J. Böttger and E.J. Mittemeijer, *Journal of Thermal Analysis and Calorimetry*, 64, pp.905-914, 2001.
[24] U.K. Viswanathan, T.R.G. Kutty and C.Ganguly, *Metall. Trans. A*, 24A, pp.2653-2656, 1993.
[25] E.J. Mittemeijer, *Journal Mater. Sci.*, 27, pp.3977-3987, 1992.
[26] De A.K., S.Vandeputte and B.C. De Cooman, *Journal of Materials Eng. and Perf.*, 10, pp.567-575(9), 2001.
[27] C.A. Wert and R.M. Thomson, Physics of Solids, McGraw-Hill, 1964.
[28] J. Mahieu, J. Maki, B.C. De Cooman and S. Claessens, *Metall. Trans. A*, pp.2573-2580, 2002.
[29] V. Burachynsky and J.R. Cahoon, *Metall. Trans. A*, 28A, pp.563-581, 1997.
[30] M.A. Wahab, Solid State Physics: Structure and Properties of Materials, Harow, 2005.